



Original Articles

JC-010a, a novel selective SHP2 allosteric inhibitor, overcomes RTK/non-RTK-mediated drug resistance in multiple oncogene-addicted cancers

Xuxiu Lu^{a,b}, Rilei Yu^{a,b}, Zhen Li^a, Mengke Yang^a, Jiajia Dai^c, Ming Liu^{a,b,*}^a Key Laboratory of Marine Drugs, Ministry of Education, School of Medicine and Pharmacy, Ocean University of China, Qingdao, 266003, China^b Laboratory for Marine Drugs and Bioproducts of Qingdao National Laboratory for Marine Science and Technology, Qingdao, 266237, China^c Key Laboratory of Marine Ecology and Environmental Sciences, Institute of Oceanology, Chinese Academy of Sciences, Qingdao, 266071, China

ARTICLE INFO

ABSTRACT

Keywords:

Acquired resistance
Cancer
NSCLC
JC-010a
SHP2

Src homology 2 domain-containing phosphatase (SHP2) is a non-receptor protein phosphatase that transduces signals from upstream receptor tyrosine kinases (RTKs)/non-RTKs to Ras/MAPK pathway. Accumulating studies indicated that SHP2 is a critical mediator of resistance to current targeted therapies in multiple cancers. Here, we reported a novel SHP2 allosteric inhibitor JC-010a, which was highly selective to SHP2 and bound at the “tunnel” allosteric site of SHP2. The effect of JC-010a on combating RTK/non-RTK or MAPK inhibitors-induced acquired resistance was explored. Our study demonstrated that JC-010a monotherapy significantly inhibited the proliferation of cancer cells with different oncogenic drivers via inhibiting signaling through SHP2. Importantly, JC-010a abolished acquired resistance induced by targeted therapies: in KRAS-mutant cancers, JC-010a abrogated selumetinib-induced adaptive resistance mediated by RTK/SHP2; in BCR-ABL-driven leukemia cells, we demonstrated JC-010a inhibited BCR-ABL T315I mutation-mediated imatinib resistance and proposed a novel mechanism of JC-010a involving the disrupted co-interaction of SHP2, BCR-ABL, and Hsp90; in non-small cell lung cancer (NSCLC) cells, JC-010a inhibited both EGFR T790M/C797S mutation and alternate RTK-driven resistance to gefitinib or osimertinib; importantly, we first proposed a novel potential therapeutic strategy for RET-rearranged cancer, we confirmed that JC-010a monotherapy inhibited cell resistance to BLU-667, and JC-010a/BLU-667 combination prolonged antitumor response both *in vivo* and *in vitro* cancer models by inhibiting the alternate MET activation-induced RAS/MAPK reactivation, thereby promoting cancer cell apoptosis. These findings suggested that JC-010a was a novel selective SHP2 allosteric inhibitor, and combining JC-010a with current targeted therapy agents provided a promising therapeutic approach for clinical resistant cancers.

1. Introduction

Protein tyrosine kinases (PTKs) constitute a class of receptor tyrosine kinases (RTKs) and non-RTKs that play important role in cancer progression [1]. The important pathways that are known to be activated by PTKs include Ras/Raf/mitogen-activated protein kinase (MAPK), Janus kinase (JAK)/signal transducer and activator of transcription (STAT), and phosphoinositide 3-kinase (PI3K)/AKT [2], which are associated with malignant transformation and tumor progression. A large number of kinase inhibitors targeting the PTK and/or MAPK pathways have been effectively used for clinical cancer treatment [3,4]. However, patients eventually develop resistance due to various mechanisms, among them, the activation of alternative RTKs [5] and the secondary mutation of the

target kinase [6,7] are the most common resistance mechanisms. Currently, even the first-line therapeutic drugs, such as gefitinib, osimertinib, and imatinib, have faced with great challenges due to acquired resistance. Therefore, it is necessary to find new drugs and/or therapeutic strategies to block the clinical drug resistance.

The Src homology 2 domain-containing phosphatase 2 (SHP2), encoded by PTPN11, composes a conserved catalytic (PTP) domain, two SH2 domains (N-SH2 and C-SH2), and a C-terminal tail [8]. SHP2 is a critical regulator of oncogenic MAPK signaling that functions in the cytoplasm downstream of multiple protein tyrosine kinases (PTKs), including RTK and non-RTK, to promote the activation of RAS/MAPK pathway [9–11], therefore, pharmacological inhibition of SHP2 may be effective for drug resistance. Early drug discovery efforts mainly focused

* Corresponding author. Key Laboratory of Marine Drugs, Ministry of Education, School of Medicine and Pharmacy, Ocean University of China, Qingdao, 266003, China

E-mail address: lmouc@ouc.edu.cn (M. Liu).

on targeting PTP, however, many reported PTP inhibitors showed low permeability and selectivity due to the negatively charged groups (e.g. sulfonic acid) to target positively charged and the high conserved environment of PTP, therefore, great efforts have been devoted to develop allosteric inhibitors [12,13]. SHP099 was the first reported SHP2 allosteric inhibitor, however, SHP099 has been proved with less efficiency compared with clinically used RTK and MAPK inhibitors; additionally, SHP099 also showed liver toxicity [12]. Thus, scientist aimed to further optimize of SHP099, currently, several SHP2 allosteric inhibitors including TNO155 (NCT03114319) [12], RMC-4630 (NCT03634982) [14], and BBP-398 (NCT04528836) [15] are in clinical trials for different types of cancer therapy. These allosteric inhibitors also demonstrated combinational benefit with MAPK inhibitors and/or RTK inhibitors. For example, TNO155 and BBP-398 in combination with the EGFR inhibitors have exhibited synergistic antiproliferative effect in NSCLC; importantly, they can overcome EGFR inhibitor-induced acquired resistance [16]. Moreover, the combination of SHP099 with MEK inhibitor can abrogate adaptive resistance to MEK inhibitors [17]. These studies strongly suggested that SHP2 allosteric inhibitors provide an appealing therapeutic approach to overcome RTK inhibitor- or MAPK inhibitor-induced acquired resistance, thereby prolonging anticancer response.

In this study, we reported the discovery of a novel and selective allosteric SHP2 inhibitor JC-010a (Table 1) via structure-based design. Compared with SHP099, the main change of JC-010a is the introduction of thiazolo ring and spirocyclic system, which contributed to the conformational stabilization and thereby improved binding affinity [12, 18]. The structure optimization elevated the inhibition activity of JC-010a both in enzymatic assay and *in vitro* antiproliferation assay (Table 1). We further evaluated the efficiency of JC-010a on various cancer cells. We then studied the capacity of JC-010a in overcoming RTK/non-RTK-mediated acquired resistance towards different tyrosine kinase inhibitors (TKIs) or MAPK inhibitors. Importantly, the *in vivo* efficiency of JC-010a was also explored in KIF5B-RET/MET-driven resistant xenograft models.

2. Materials and method

2.1. Drugs and reagents

JC-010a (purity >99%) was synthesized by Alta Scientific Co., Ltd., Tianjin, China. Selumetinib and osimertinib were purchased from Sell-eckchem (Shanghai, China). SHP099 was obtained from Bidepharm (Shanghai, China). SPI-112 was obtained from TOPSCIENCE (Shanghai, China). Pralsetinib was obtained from MedChemExpress. Antibodies against phospho-ERK, phospho-MEK, phospho-AKT, and SHP2 were obtained from Cell Signaling Technology (Boston, MA, USA). Phospho-SHP2 was obtained from Abcam (Cambridge, MA, USA). Tubulin and

GAPDH antibody were purchased from Huaan Biotechnology Co., Ltd. (Hangzhou, China).

2.2. Cell culture and generation of engineered lines

K562, A549, MIAPaCa-2, H358, PC-9, and KYSE-520 were purchased from China Center for Type Culture Collection (CCTCC), imatinib-resistant K562 cell line K562/r was purchased from American Type Culture Collection (ATCC). PC-9/GR was obtained from Shanghai Yaji Biotechnology Co., Ltd. BaF3/BCR-ABL^{WT} and BaF3/BCR-ABL^{T315I} cells were obtained from Cobioer Biosciences Co., Ltd., Nanjing, China. BaF3/CCDC6-RET and BaF3/KIF5B-RET cell lines were provided by Shanghai Institute of Materia Medica, Chinese Academy of Sciences. All cell lines were cultured in RPMI1640 Medium (ExCell Bio) except MIAPaCa-2 (DMEM) and KYSE-520 (DMEM) supplemented with 10% FBS (Gibco, USA) and 1% penicillin/streptomycin at 37 °C in a humidified incubator containing 5% CO₂. All cell lines used were determined to be free of mycoplasma contamination. And cell lines were used within 3–10 passages of thawing and continuously cultured for less than 2 months.

BaF3/CCDC6-RET and BaF3/KIF5B-RET cell lines overexpressing MET were generated by infecting with lentiviruses generated from empty pCDH-CMV-EF1 lentiviral vector or pCDH-CMV-EF1 vector containing a MET cDNA. Stable MET overexpressing cells were selected using the Hygromycin B.

PC-9 cells that harbored EGFR^{T790M/C797S} mutation were generated using site-directed mutagenesis method using the following primers (5'-3'): F1: accatggccatcgtagctagcATGCGACCCTCGGGACG; R1: tggttagccgtaccctcgagTGCTCCAATAATTCACTGCTTTG; F2: ctcacccatcgctgcagctcatcatgcagctcatgccttcggctcccttgactatgtccggaaacac; R2: gtgttccggacatgtccaggaggagccgaaggcatgagctgcatgtgatgagctgcacggtgagggtgg. The detailed methods information is provided in Supplementary Information. Viruses were produced by co-transfected HEK293T cells with lentiviral and packaging vectors. The PC-9 infected cells were selected beginning 48 h post-infection using Hygromycin B.

2.3. Cell viability assay

The effect on cell proliferation of JC-010a (dissolved in DMSO) alone or in combination with other drugs was tested by 3-(4,5-dimethylthiazol-2-yl)-2,5-diphenyltetrazolium bromide (MTT) method. For colony formation assay, cells (500–800) were seeded in 6-well plates and treated with indicated drugs, and colonies were stained with crystal violet. For Soft agar colony formation assay, 6-well plates were first coated with 1.2% agarose, then cells were mixed with the DMEM containing 0.4% agarose and indicated drugs, finally, the mixture immediately overlaid on the pre-coated plates. The culture medium was changed every 3 d.

Table 1
Inhibitory effect of SHP099 and JC-010a.

Compound	Structure	SHP2 IC ₅₀ (nM)	Antiproliferation IC ₅₀ (μM)
SHP099		316.38 ± 29.06	15.26 ± 1.67
JC-010a		56.94 ± 4.75	0.48 ± 0.03

Noted: KYSE-520 cells were used for antiproliferation assay.

2.4. Western blotting assay

The harvested cells were washed with ice-cold PBS and lysed with lysis buffer containing a protease inhibitor cocktail. Proteins were separated by SDS-polyacrylamide gels, and then transferred to nitrocellulose membranes. The membrane was blocked in 5% skim milk for 1 h and incubated with corresponding primary antibodies overnight at 4 °C, and then the membranes were incubated with secondary antibody at room temperature for 1 h and detected by Tanon 5200 (Tanon, Beijing, China).

2.5. Flow cytometric assay

The effect of JC-010a alone or in combination with other drugs on cell cycle distribution was detected by flow cytometry using PI staining and analyzed by ModFit LT software (Versity Software House). Apoptosis was quantified by using the Annexin V-FITC apoptosis detection kit according to previous studies [19].

2.6. Hoechst 33342 staining

Cells were seeded at 12-well plates and treated with JC-010a alone or in combination with indicated drugs. Cells were fixed, stained, and finally observed with a fluorescent microscopy (Leica, Germany).

2.7. In vitro enzymatic assay

To study the effect of JC-010a on the phosphatase activity of full-length human SHP2 (Bioscience, San Diego, CA, USA), fluorogenic 6,8-difluoro-4-methylumbelliferyl phosphate (DiFMUP; Bioscience) was used as the substrate. Briefly, the full length SHP2 protein was incubated with indicated compound and activating peptide in assay buffer at room temperature for 1 h. Then the substrate DiFMUP was added to initiate the reaction. After 30 min, the DiFMU fluorophore was measured (Ex:360/Em:455) using SpectraMax® i3x multi-mode microplate reader (Molecular Devices, San Jose, CA, USA). The phosphatase activity of SHP2 phosphatase domain was conducted using SHP2₂₃₇₋₅₂₉, and the para-nitrophenyl phosphate (pNPP) disodium was used as substrate, and measured at 405 nm. The phosphatase activity of PTP1B and SHP1 were performed in a similar method.

2.8. Protein expression and purification of SHP2₂₃₇₋₅₂₉

The human SHP2₂₃₇₋₅₂₉ gene were cloned into the prokaryotic expression vector (pET-30a(+)). The recombinant plasmids were transformed into BL21 (DE3) bacteria and cultured containing 50 µg/mL kanamycin. When the OD₆₀₀ reached 0.6–0.8, isopropyl-β-D-thiogalactopyranoside (IPTG) was added to induce SHP2 expression, and then bacteria were harvested after growth for 24 h at 18 °C.

The pellets were re-suspended in lysis buffer (50 mM Hepes, 5 mM imidazole, 5% Glycerol, 500 mM NaCl at pH 7.5) and lysed on ice by sonication. The supernatant was collected and loaded onto a column containing 2 mL of Ni-NTA-agarose resin. The column was eluted with column buffer containing 5–200 mM imidazole. The protein was concentrated using Amicon Ultra centrifugal concentrators (Millipore).

2.9. Surface plasmon resonance (SPR) assay

To analyze the interaction between JC-010a and SHP2, SPR experiments were performed using Biacore T200 (GE Healthcare). SHP2 protein was firstly immobilized on the CM5 chip by Amine Coupling Kit (BR-1000-50, GE Healthcare). Briefly, PBS-P running buffer was used to wash the surface of the chip, and then the chip was activated by injecting EDC/NHS. After activation, SHP2 protein was diluted with sodium acetate buffer (10 mM, pH 5.0) and immobilized on the chip. Ethanolamine (1 M, pH 8.5) was used to block the unreacted, activated

carboxylic acids on the chip surface. Compounds were dissolved to a concentration of 10 mM in DMSO and then diluted in PBS-P buffer. The response was monitored as a function of time at 25 °C and subtracted the reference data and blank data using the Biacore T200 Evaluation Software, and curve-fitting (global fitting, 1:1 model) was performed for the whole kinetic parameters.

2.10. Molecular docking

Molecular docking was performed using AutoDock Vina. The crystal structures of SHP2 (PDB ID: 5EHR) was optimized including removal of water molecules, addition of polar hydrogen atoms, and charge assignment using AutoDock Tools; and the ligand was protonated at physiological pH prior to docking using ChemOffice Suite and AutoDock Tools. Finally, JC-010a was docked into the pocket of SHP2, and the composite structure with top-scored and reasonable conformation was selected. The proposed binding mode was analyzed by PyMOL.

2.11. Co-immunoprecipitation (Co-IP)

Co-IP was performed using protein A/G agarose according to manufacturer's instructions. Briefly, pretreated cells were lysed in IP lysis buffer and centrifuged. Then, the supernatants were incubated with protein A/G agarose and indicated antibody. And rabbit IgG was used as a control. Finally, the precipitates were washed and eluted with loading buffer for further immunoblotting.

2.12. In vivo antitumor study of JC-010a

BALB/c nude mice (6-week-old, female) were purchased from Beijing Vital River Laboratory Animal Technology Co., Ltd. To establish BaF3/KIF5B-RET/MET xenografts, 5 × 10⁶ of cells were implanted subcutaneously into the right flank of mice. Mice were divided into 5 groups and treated with JC-010a (20 mg/kg, QD, p.o.), BLU-667 (30 mg/kg, BID, p.o.), SHP099 (60 mg/kg, QD, p.o.), or combination of JC-010a and BLU667 for 12 consecutive days; the vehicle group received the equivalent volume of NMP and Solutol HS-15. The tumor volume and mouse body weight were recorded every other day, and the tumor volume was calculated by the following formula: length × width²/2. Finally, mice were sacrificed and the tumor tissues were weighted. Tumor growth inhibition (TGI) were calculated as follows: TGI = 100% × [1 – (TV_t(T) – TV_{initial}(T))/(TV_t(C) – TV_{initial}(C))], in which TV_{initial}(T) and TV_t(T) are the tumor volumes before administration and final time in the drug treatment group, respectively, and TV_{initial}(C) and TV_t(C) are the tumor volumes in vehicle group. Animal experiments were approved by the Institutional Animal Care and Use Committee of the Ocean University of China (No.OUC-SMP-2022-08-02).

Tumor tissues and the viscus were collected and processed into paraffin for hematoxylin and eosin (H&E) staining.

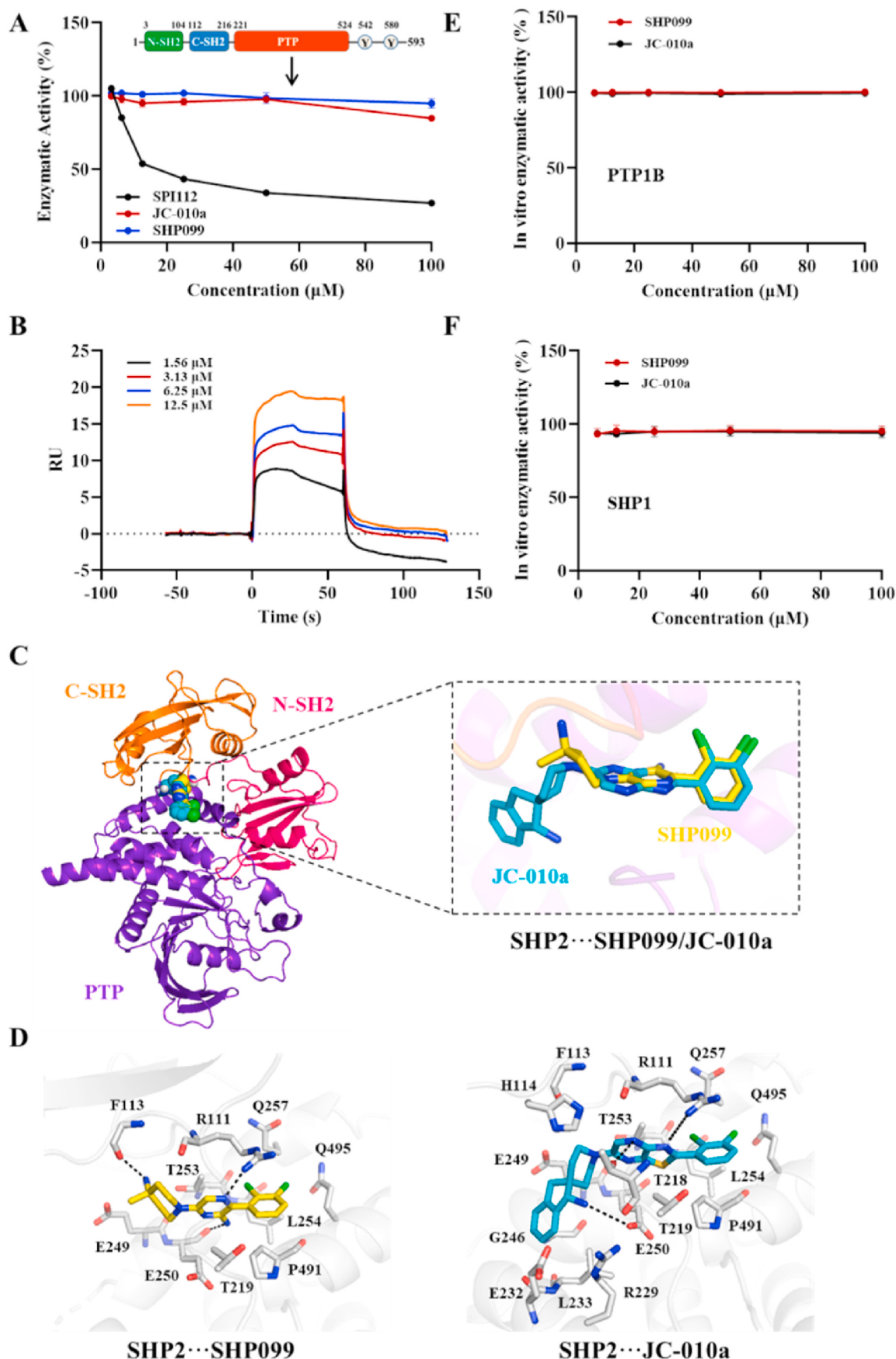
2.13. Statistical analysis

The results are presented as mean values ± SD. Two groups were compared using a two-tailed Student's t-test. Comparisons between multiple groups were performed using a one-way analysis of variance (ANOVA) followed by multiple comparisons Tukey test. *P* < 0.05 was defined statistically significant.

3. Results

3.1. JC-010a is a selective allosteric inhibitor of SHP2

In an *in vitro* enzymatic assay, JC-010a suppressed the phosphatase activity of full-length human SHP2 protein, with an IC₅₀ value of 56 nM (Table 1). SHP2 phosphatase domain was further used to investigate the impact of JC-010a on SHP2. As shown in Fig. 1A, JC-010a had no



(caption on next page)

Fig. 1. JC-010a is a selective allosteric SHP2 inhibitor. (A) The effect of JC-010a on the enzyme activity of the SHP2 phosphatase domain. SPI112 was used as positive control, and SHP099 was served as negative control. The assays were replicated three times, the data are represented as the mean \pm SD. (B) The binding affinity of JC-010a and full-length SHP2 was analyzed by the SPR. (C) Binary complex model of SHP2···JC-010a and SHP2···SHP099, and structural overlay of JC-010a and SHP099. The N-SH2, C-SH2, and the PTP domain of SHP2 are presented by hot pink, orange, and purple cartoons, respectively. The compounds JC-010a and SHP099 are shown in cyan and yellow stick. (D) The interaction details of SHP2 with SHP099 (left) and JC-010a (right). Key residues are presented by gray bars. Hydrogen bonds are indicated by black dashed lines. (E, F) Effect of JC-010a on the enzyme activity of the PTP1B and SHP1. The assays were replicated three times, the data are represented as the mean \pm SD.

obvious effect on phosphatase activity even at concentrations of 100 μ M, and the dissociation constant (K_D) of JC-010a binding to full-length SHP2 was about 0.69 μ M, as shown by the surface plasmon resonance (SPR) analysis (Fig. 1B), demonstrating JC-010a was an effective allosteric inhibitor of SHP2. To explore the possible binding mode of JC-010a with SHP2, JC-010a was docked into the allosteric binding site of SHP2 (PDB: 5EHR). Our results revealed that JC-010a and SHP099 shared similar binding patterns (Fig. 1C). Compared with SHP099, several new interactions between JC-010a and SHP2 were observed (Fig. 1D). We found that the N atom of the thiazol ring of JC-010a formed a hydrogen bond with the side chain NH₂ of SHP2 R111. Importantly, the pyrazine N and the NH₂ group of spiro in JC-010a formed hydrogen bonding interactions with the side chain hydroxyl of SHP2 T218 and side chain carbonyl of E250, respectively. In addition to the 3 hydrogen bonds, the extensive hydrophobic interactions with F113, T219, L254, Q257, P491, Q495, etc, contributing to the stabilization of the whole binding system. Interestingly, multiple interactions between the residue of the other side of the allosteric pocket and the extended spiro of JC-010a were observed. And these newly formed interactions may explain the increased inhibitory activity of JC-010a compared with SHP099. To determine the selectivity of JC-010a, the inhibitory activity against SHP1 and PTP1B were measured. As shown in Fig. 1E and F, JC-010a displayed excellent selectivity toward SHP2 with IC₅₀ values over 100 μ M among the tested PTPs. It should be noted that JC-010a demonstrated no inhibition on the full-length SHP1 (Fig. 1F), which shows 75% amino acid sequence similarity with SHP2. Collectively, these results indicated that optimized JC-010a was a selective allosteric SHP2 inhibitor, and the efficiency was higher than SHP099.

3.2. JC-010a prevents adaptive resistance to MEK inhibitors in KRAS-mutant cancers due to on-target effect

MEK inhibitors serve as one of approaches to treat KRAS-mutant cancers [20], however, the multiple RTKs activation, such as EGFR, FGFR3, IGFR1, MET, and PDGFRB, contribute to the adaptive resistance to MEK inhibitor [17]. In this regard, it is difficult to identify an efficient combination therapy with MEK inhibitor to target certain RTKs directly. SHP2 acts as a convergent node between multiple RTKs/non-RTKs and RAS, therefore, the combination of JC-010a and MEK inhibitor may be effective to prevent adaptive resistance. We then treated KRAS-mutant cancer cells with JC-010a and selumetinib (AZD6244), our results revealed that selumetinib treatment reactivated ERK upon treatment for 12 h in A549 cells, and SHP2 inhibition by JC-010a prevented the reactivation of ERK (Fig. 2A), as well as the MEK phosphorylation (Fig. 2A). We next used KRAS^{G12C} mutation cell models to further analyze the effect of JC-010a on selumetinib-induced adaptive resistance, as KRAS^{G12C} has the highest intrinsic GTP hydrolysis activity among all KRAS mutants [21]. Our results revealed that selumetinib treatment, as early as 2 h, induced obvious reactivation of MEK in MIAPaCa-2 cells and H358 cells (Fig. 2B and C), and JC-010a treatment inhibited the rebound of p-ERK and p-MEK (Fig. 2B and C), indicating JC-010a could abrogate SHP2-mediated adaptive activation induced by selumetinib. Our results also revealed that in the presence of 2% FBS, selumetinib-induced adaptive resistance was less pronounced than that in 10% FBS, and JC-010a treatment resulted in nearly complete inhibition of p-MEK and p-SHP2 (Fig. S1), suggesting JC-010a could efficiently impede RTK/SHP2-mediated adaptive resistance. Collectively, these results indicated that JC-010a significantly abrogated

selumetinib-induced adaptive resistance.

To explore whether SHP2 inhibition by JC-010a could sensitize cells to selumetinib, we analyzed the combination index and performed colony formation assays on KRAS-mutant cell lines. In A549 cells, JC-010a showed moderate effect, whereas there were no detectable colonies in combination treatment group (Fig. 2D). In KRAS G12C mutant cells, JC-010a, either used as single agent or in combination with selumetinib, obviously reduced cell numbers with few or no detectable colonies in these 2 cell lines (Fig. 2E and F); also JC-010a exhibited strong synergy with selumetinib in KRAS^{G12C} cells, evidenced by the combination index (CI) < 1 (Fig. 2G and H), suggesting JC-010a could sensitize KRAS-mutant cells to selumetinib. And the combination treatment arrested cell cycle at G2/M phase (Figs. S2A and B) in MIAPaCa-2 cells, which further confirmed JC-010a and selumetinib combination synergistically inhibited cell growth. Our results also indicated that KRAS-mutant cell lines exhibited low sensitivity to SHP099 compared to JC-010a (Fig. 2D–F), suggesting the enhanced activity after structural optimization of JC-010a. Collectively, these results indicated that JC-010a efficiently abolished selumetinib-induced adaptive resistance and sensitized cells to selumetinib.

To ensure that the anti-proliferation and signaling inhibition effect of JC-010a was due to inhibition of SHP2, we stably established H358 cells with SHP2 knockdown. Our results indicated that the signaling inhibition effect of JC-010a was abolished in H358 cells with SHP2 knockdown compared to scrambled control (Fig. 2I). Similarly, knockdown of SHP2 significantly reduced the anti-proliferation effect of JC-010a (Fig. 2J). Collectively, these results indicated that JC-010a-induced suppression on cell proliferation and MAPK signaling pathways were due to its inhibition effect on SHP2.

3.3. JC-010a overcomes BCR-ABL^{T315I}-mediated imatinib resistance by disrupting the interaction between SHP2, BCR-ABL, and Hsp90

CML is characterized by the constitutively activated of BCR-ABL tyrosine kinase [22]. Imatinib has been approved for the therapeutic drug for CML in clinic, however, BCR-ABL T315I mutation limited the clinical outcomes of imatinib [23,24]. At present, none of a report has studied the effect of SHP2 allosteric inhibitors in overcoming imatinib resistance in CML, as well as the related mechanisms. SHP2 has been identified as a require node for BCR-ABL leukemogenesis [10]. Our bioinformatic analysis revealed that ABL and SHP2 have high positive correlations in CML patients (Fig. 3A). Thus, we speculated that pharmacological inhibition of SHP2 might overcome BCR-ABL T315I-mediated imatinib resistance. Subsequently, we investigated the effects of JC-010a on CML cells. K562 and BaF3/BCR-ABL^{WT} cells are sensitive, whereas K562r and BaF3/BCR-ABL^{T315I} cells are resistant to imatinib treatment (Fig. 3B). Our results indicated that JC-010a showed similar inhibition potency in imatinib-sensitive and imatinib-resistant cells, with IC₅₀ values of 2.6, 2.4, 4.1, and 5.1 μ M (Fig. 3C), in K562, K562r, BaF3/BCR-ABL^{WT}, and BaF3/BCR-ABL^{T315I} cell, respectively. Similarly, *in vitro* clonogenic assay, JC-010a significantly reduced the colonies of CML cells (Fig. 3D), indicating JC-010a showed similar activity in imatinib-sensitive and imatinib-resistant cells. Our results also demonstrated that JC-010a showed superior inhibition activity to SHP099 in the proliferation of CML cells (Fig. S3). Taken together, these results indicated that JC-010a was able to overcome BCR-ABL T315I mutation-induced imatinib resistance in CML.

Due to the high positive correlations of SHP2 and BCR-ABL, we then

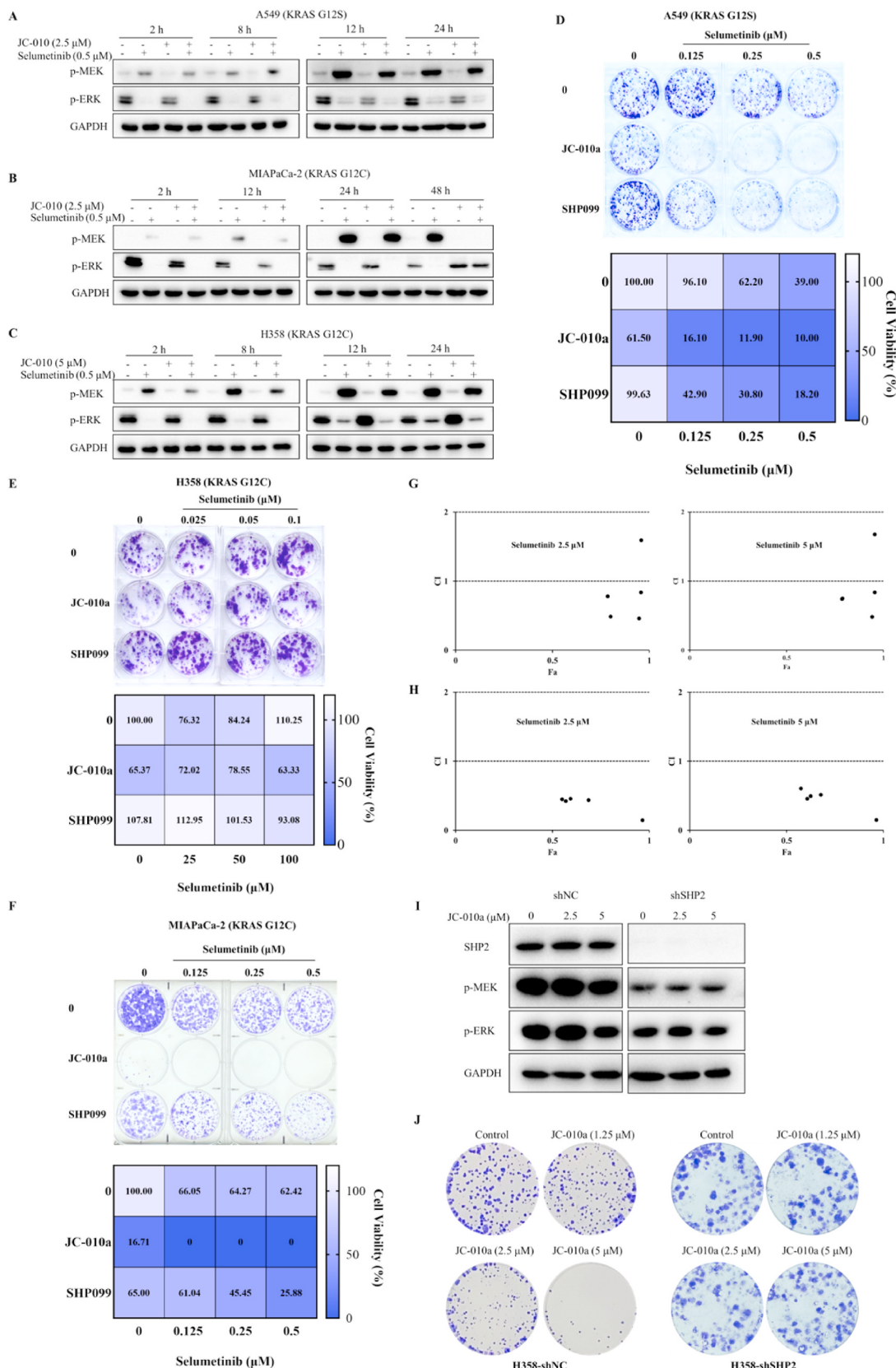
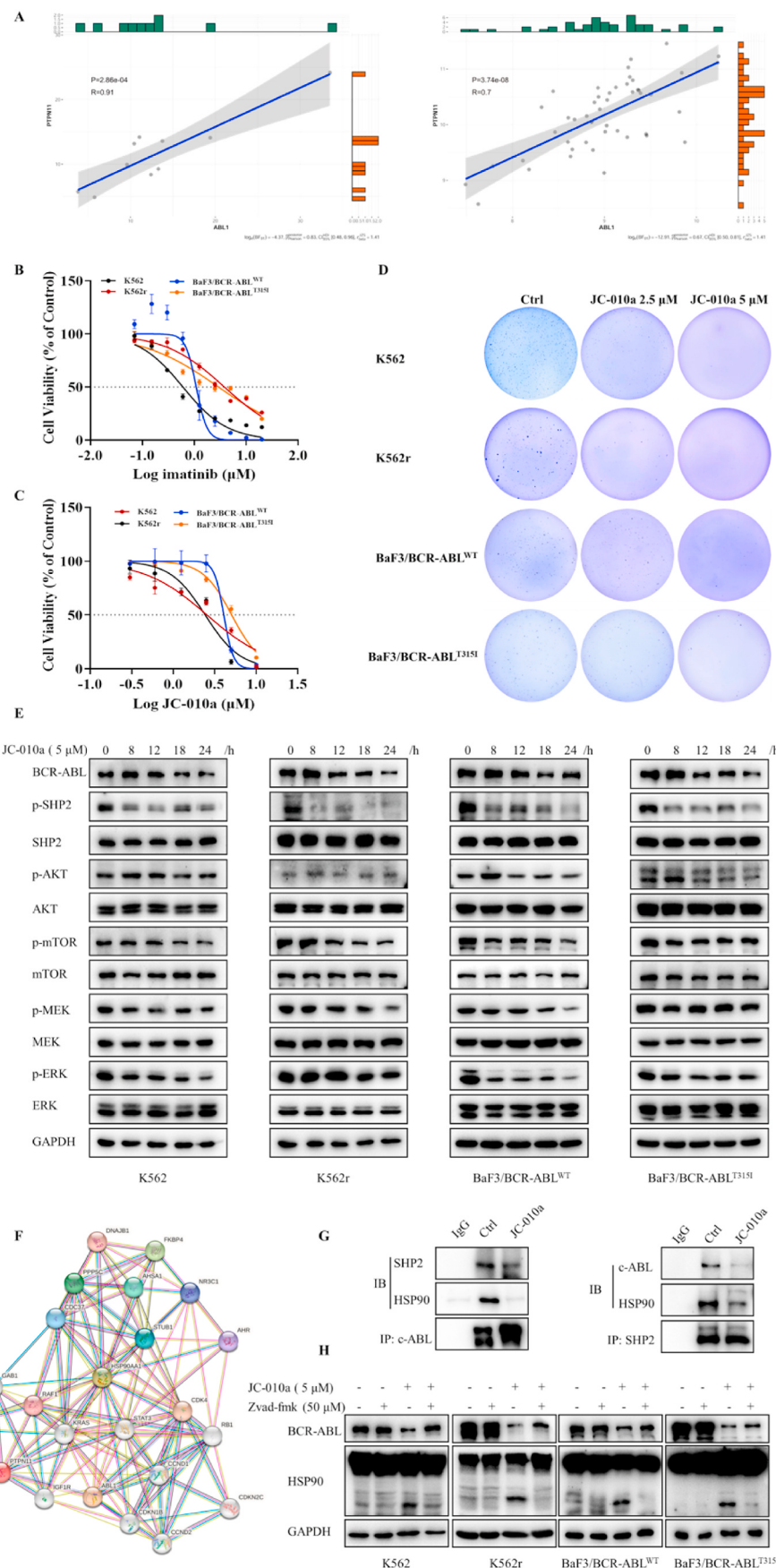


Fig. 2. JC-010a overcomes selumetinib-induced adaptive resistance in KRAS-mutant cells due to on-target effect. JC-010a abolishes SHP2-mediated adaptive resistance to selumetinib in A549 (A), MIAPaCa-2 (B), and H358 cells (C). Antiproliferative activity of JC-010a in combination with selumetinib in A549 (D), H358 (E), and MIAPaCa-2 cells (F). The combination effect was studied to determine the synergistic effects of JC-010a and selumetinib in MIAPaCa-2 (G) and H358 cells (H). The CI values of >1 , $=1$, and <1 indicate antagonistic, additive, and synergistic effects, respectively. Fa indicated the fractions of the affected cells. (I) Effect of JC-010a (3 h) on the phosphorylation of ERK and MEK in H358 cells with normal level SHP2 or SHP2 knockdown. (J) Effect of JC-010a on the colony formation of cells in I.



(caption on next page)

Fig. 3. JC-010a overcomes BCR-ABL-dependent imatinib resistance in CML cells by disrupting the co-interaction between SHP2, BCR-ABL, and Hsp90. (A) Correlation between the mRNA level of ABL1 and PTPN11 in CML patient from the RNA-seq dataset (GSE100026 and GSE144119). CML cells were treated with various concentrations of imatinib (B) and JC-010a (C) for 72 h, and cell viability was determined by MTT assay. (D) *In vitro* soft agar colony formation analysis the long-term effect of JC-010a on CML cells treated for 14 d. (E) Western blotting analysis of BCR-ABL and its downstream targets in CML cells that were treated with 5 μ M of JC-010a for indicated time. (F) Protein-protein interaction network analysis. (G) Pharmacological inhibition of SHP2 induced by JC-010a disrupts the co-interaction between BCR-ABL, Hsp90, and SHP2. K562 cell was treated JC-010a (5 μ M) for 24 h, cell lysates were immunoprecipitated (IP) with *anti*-ABL or *anti*-SHP2. (H) Pan caspase inhibitor Zvad-fmk attenuates JC-010a-induced BCR-ABL degradation and Hsp90 cleavage. CML cells were pretreated with Zvad-fmk for 2 h followed by incubation with JC-010a for 24 h, cell lysates were subjected to western blotting.

explored whether inhibition of SHP2 could affect BCR-ABL and thereby suppress proliferation of CML cells. Our results revealed that JC-010a downregulated the expression levels of BCR-ABL both in imatinib-sensitive and imatinib-resistant CML cells (Fig. 3E), correspondingly, JC-010a inhibited the activation of BCR-ABL downstream signaling pathways, and the phosphorylation of MEK and ERK were significantly decreased, while JC-010a had moderate effect on AKT/mTOR pathway. Our results indicated that in the presence of cycloheximide, JC-010a dramatically decreased BCR-ABL protein level (Fig. S4), indicating that JC-010a-mediated BCR-ABL downregulation was on the post-translational level. Collectively, these results indicated that SHP2 inhibition by JC-010a lead the decrease of BCR-ABL expression and consequently its downstream signaling pathway, thereby inhibiting the proliferation of CML cells.

To gain insight into the mechanisms of SHP2 inhibition mediated by JC-010a could induce BCR-ABL decrease, a protein-protein interaction network was analyzed. As shown in Fig. 3F, we found a co-interactor of BCR-ABL and SHP2, heat shock protein 90 (Hsp90), which was an essential chaperone in protein folding and the function of its client protein, including BCR-ABL [25]. Therefore, we hypothesized that JC-010a might interfere the co-interaction of BCR-ABL, Hsp90, and SHP2, leading to the instability of BCR-ABL. To validate this hypothesis, we examined the co-interaction between BCR-ABL, Hsp90, and SHP2. The results suggested that JC-010a destroyed the co-interaction between BCR-ABL, SHP2, and Hsp90 (Fig. 3G), implying that SHP2 inhibition by JC-010a promoted the instability of BCR-ABL, thereby promoting BCR-ABL degradation. Since caspase activation was involved in BCR-ABL degradation pathway [26], we next explored whether JC-010a-induced BCR-ABL degradation was dependent on caspase activation. As shown in Fig. 3H, pan-caspase inhibitor Zvad-fmk could restore JC-010a-mediated the decrease of BCR-ABL, suggesting that caspase activation was required for BCR-ABL degradation. We also found that Hsp90 was cleaved to a 55 kDa protein after JC-010a treatment, and the cleavage of Hsp90 was obviously attenuated by Zvad-fmk (Fig. 3H), suggesting that caspase activation also promoted Hsp90 cleavage and further decreased the co-interaction with SHP2 and BCR-ABL. In addition, we also found SHP099 (5 μ M) showed no effect on BCR-ABL degradation (Fig. S5), demonstrating the advantage of JC-010a over SHP099. Taken together, these results indicated that JC-010a-induced the disruption of the SHP2, BCR-ABL, and Hsp90 contributed to BCR-ABL oncoprotein degradation, ultimately overcoming BCR-ABL T315I-mediated imatinib resistance.

3.4. JC-010a overcomes EGFR-dependent and EGFR-independent resistance towards EGFR inhibitors

Several generations of EGFR TKIs such as erlotinib, gefitinib, and osimertinib, have been developed for the first-line treatment of NSCLC, yet EGFR T790M and/or C797S mutation-mediated acquired resistance to gefitinib/erlotinib and osimertinib is ubiquitous and remains a key challenge [27]. SHP2 was the downstream of EGFR, thus, the efficiency of SHP2 inhibitor was not affected by the mutations of upstream RTKs. We deduced that JC-010a might have efficiency in tumors harboring EGFR T790M/C797S mutations. Therefore, we established PC-9^{T790M/C797S} cell line, the results indicated that PC-9^{T790M/C797S} cells were significantly resistant to gefitinib and osimertinib (Fig. 4A and B), we also found osimertinib could not completely inhibit the levels of

p-ERK or *p*-MEK even at 200 nM in PC-9^{T790M/C797S} cells (Fig. 4B) compared with its parental cells. However, both PC-9 and PC-9^{T790M/C797S} cells showed similar potency to JC-010a (Fig. 4C), demonstrating JC-010a overcame EGFR T790M and/or C797S-induced acquired resistance to gefitinib and osimertinib.

In addition to gatekeeper mutations in EGFR, alternative RTK activation have accounted for another common acquired resistance mechanism of EGFR TKIs [28,29]. We next examined whether JC-010a have inhibition effect in gefitinib-resistant PC-9 cells (PC-9/GR) with MET amplification. As shown in Fig. 4D and E, PC-9/GR cells showed the reduced sensitivity to gefitinib and osimertinib. Intriguingly, JC-010a showed the similar inhibition effect in PC-9 and PC-9/GR cells (IC₅₀: PC-9 = 5.4 μ M, PC-9/GR = 6.0 μ M, Fig. 4F); importantly, JC-010a sensitized cells to gefitinib in both PC-9 and PC-9/GR cells (Fig. 4G), indicating JC-010a impeded alternate RTK-induced resistance and sensitized cells to gefitinib. Collectively, these results indicated that JC-010a can efficiently overcome both EGFR mutations (T790M and/or C797S) and alternate RTK-induced resistance to gefitinib and osimertinib in NSCLC.

3.5. JC-010a abrogates BLU-667-induced acquired resistance and sensitizes cells to BLU-667 in RET rearranged cells

Rearranged during transfection (RET) gene rearrangements triggers ligand-independent, constitutive RET kinase activation, which promotes tumorigenesis [30]. The approved highly potent and RET-specific inhibitors pralsetinib (BLU-667) was successfully translated to the clinic [31]. In our present study, we found BLU-667 treatment for 2 h resulted in dramatic decrease of phosphorylation of MEK, ERK, and AKT in KIF5B-RET and CCDC6-RET fusion cells (Fig. 5A and B), however, this effect was successively abolished after 12, 18, and 24 h treatment, and the reactivation of MEK, ERK, and AKT were found (Fig. 5A and B). Surprisingly, JC-010a co-treatment blocked the rebound of MEK and ERK phosphorylation in response to BLU-667 in KIF5B-RET and CCDC6-RET fusion cells (Fig. 5C and D); additionally, our results also indicated that the activity of JC-010a was much better than SHP099 in preventing the reactivated signaling pathway (Fig. 5C), which was consistent with the results observed in KRAS-mutant cells. We next explored whether JC-010a could have synergism with BLU-667, and our results demonstrated that the combination was synergistic in most tested concentrations (Fig. 5E). Consistently, there are few colonies after JC-010a and BLU-667 combination treatment than single treatment (Fig. 5F), which showed excellent synergy effect (Fig. 5F). Also, the drug combination enhanced cell apoptosis (Figs. S6A and B) and decreased cell cycle progression (Figs. S6C and D) compared with either single drug alone. Taken together, these observations exhibited that JC-010a abolished BLU-667-induced pathway reactivation and also increased efficiency of BLU-667 in RET-fusion cancer cells.

One common reported alternative RTK activation is the MET amplification, which is accounted for the majority of resistance to selective RET inhibition [32], we then overexpressed MET in RET fusion cells to test the activity of JC-010a in BLU-667-resistant cells with alternate RTK activation. The results indicated that MET-overexpressed RET rearranged cells were far less sensitive to BLU-667 (Fig. 5G and H). However, JC-010a suppressed the proliferation of both the parental and MET overexpression cells with similar potency (Fig. 5I). Consistent with observations in parental cells (Fig. 5E and F), JC-010a treatment

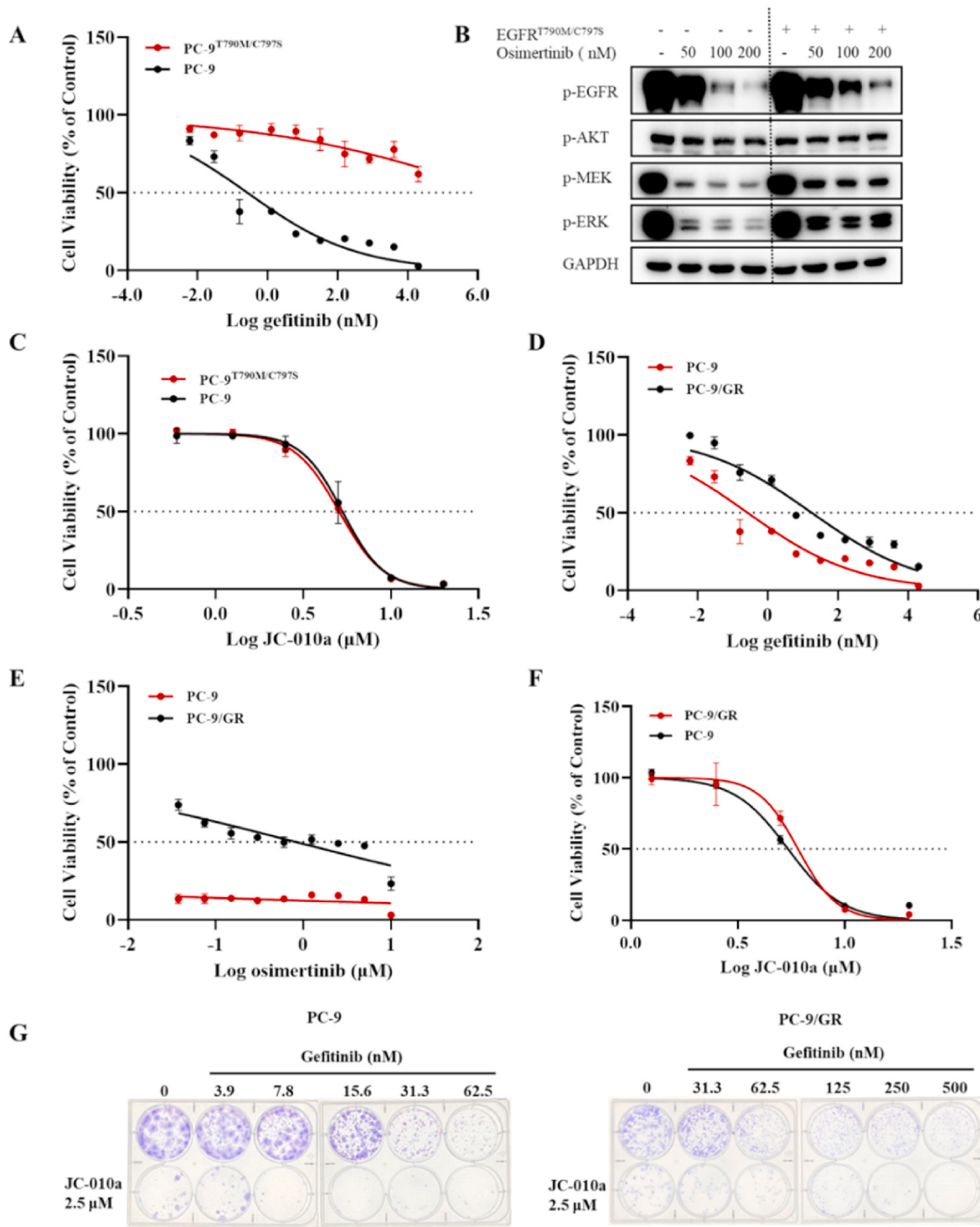
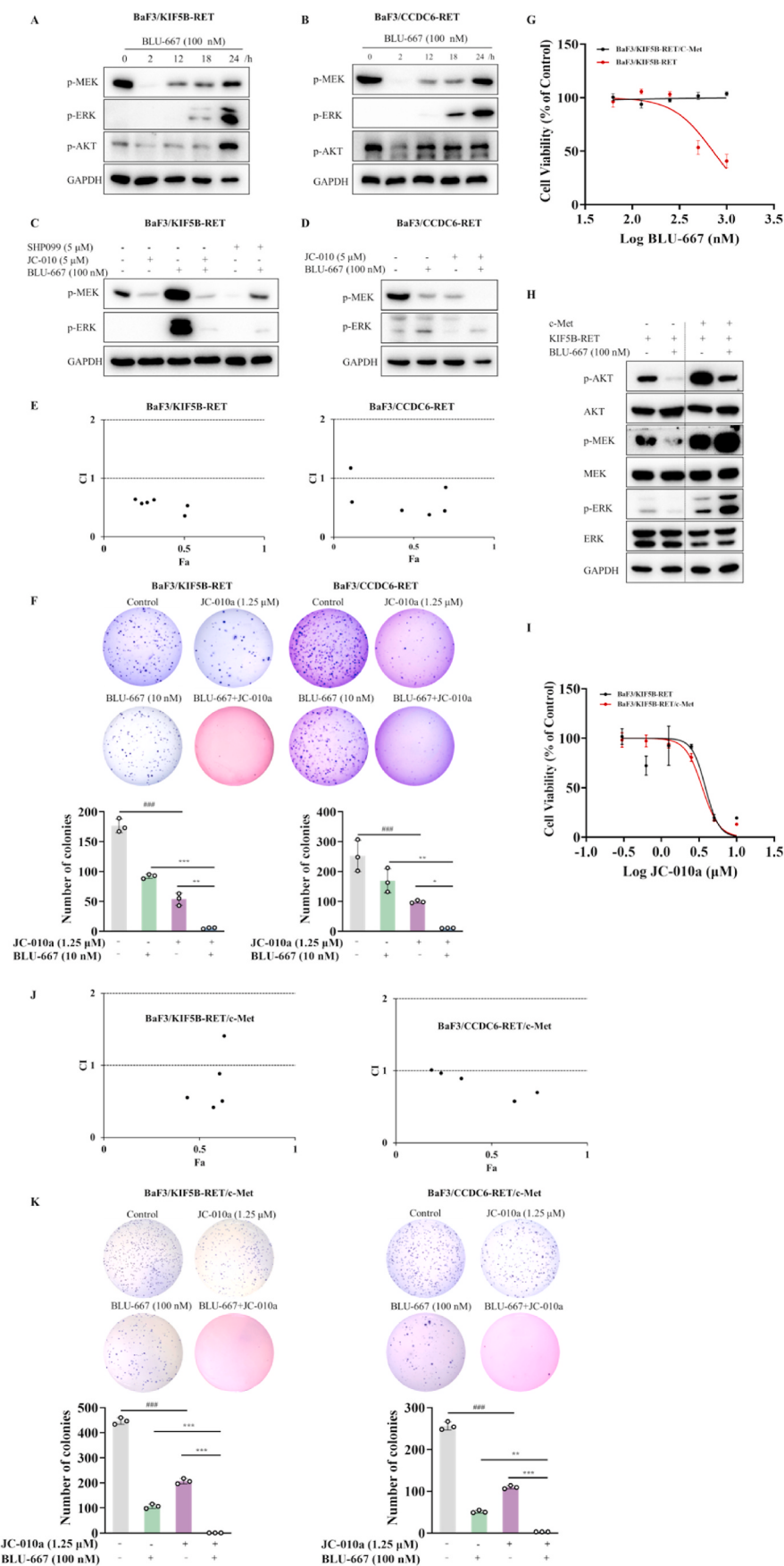


Fig. 4. JC-010a suppresses the proliferation of EGFR TKI-resistant NSCLC cells and demonstrates combination benefits with EGFR TKI. (A) Effect of gefitinib on the proliferation of PC-9 cells and PC-9 cells overexpressing EGFR^{T790M/C797S}. (B) Immunoblot of PC-9 and PC-9^{T790M/C797S} cells that were treated with osimertinib for 2 h. (C) The proliferation of PC-9 and PC-9^{T790M/C797S} cells that were treated with JC-010a for 72 h. Effect of gefitinib (D), osimertinib (E), and JC-010a (F) on the proliferation of PC-9 cells and PC-9 cells harboring RTK-bypass. (G) Combination effect of JC-010a and gefitinib on PC-9 and PC-9/GR cells treated for 12 d. Data are presented as mean \pm SD ($n = 3$).

inhibited the colony formation of MET overexpression cells, and the combination of JC-010a and BLU-667 also resulted in a synergistic antiproliferative effect on MET overexpressed cells (Fig. 5J and K); similarly, SHP2/RET co-inhibition synergistically promoted apoptosis (Figs. S7A and B), suggesting JC-010a was highly efficacious in overcoming acquired resistance to BLU-667 mediated by MET activation.

Taken together, these results demonstrated that JC-010a suppressed alternate MET activation-induced acquired resistance to BLU-667 and increased efficiency of BLU-667 *in vitro*.



(caption on next page)

Fig. 5. JC-010a inhibits alternate MET activation-induced resistance to BLU-667 in RET rearranged cells. Effect of BLU-667 in KIF5B-RET (A) and CCDC6-RET (B) fusion cells. RET rearranged cells were treated with BLU-667 (100 nM) and JC-010a (5 μ M) for 18 h, and the alternations of MEK and ERK were detected in KIF5B-RET (C) and CCDC6-RET (D) fusion cells. SHP099 was served as positive control. (E) JC-010a has synergism effect with BLU-667. Cells were treated with JC-010a (2 μ M) and various concentrations of BLU-667 for 48 h, the CI was calculated by median effect plot analysis. (F) *In vitro* clonogenic assay to determine the effect of JC-010a in combination with BLU-667 in KIF5B-RET and CCDC6-RET fusion cell lines. (G) The effect of BLU-667 on the proliferation of MET overexpressed BaF3/KIF5B-RET cells and its parental cell lines. (H) Change of signaling pathway in KIF5B-RET fusion cells overexpressing MET that were treated with BLU-667 for 2 h. (I) Effect of JC-010a on the proliferation of BaF3/KIF5B-RET and BaF3/KIF5B-RET/c-MET cells. (J) JC-010a is synergistic with BLU-667 in BaF3/KIF5B-RET/c-MET and BaF3/CCDC6-RET/c-MET cells. (K) *In vitro* clonogenic assay to evaluate the combination effect of JC-010a and BLU-667 in MET overexpressed KIF5B-RET and CCDC6-RET fusion cell lines. Data are presented as mean \pm SD ($n = 3$). $^{###}P < 0.001$, versus control group; $^{***}P < 0.001$, $^{**}P < 0.01$, versus BLU-667 or JC-010a group.

3.6. JC-010a overcomes RET-independent drug resistance and enhances the efficiency of BLU-667 *in vivo*

To evaluate the *in vivo* efficiency of JC-010a in overcoming alternate MET activation-induced resistance in RET-rearranged tumors, we treated mice bearing KIF5B-RET/MET subcutaneous xenografts with JC-010a, BLU-667, or both of them for 12 d (Fig. 6A). JC-010a (20 mg/kg, QD), 3 times less than the dose of SHP099 (60 mg/kg, QD), obviously inhibited tumor growth, with tumor growth inhibition (TGI) value of 45.4%, while SHP099 showed moderate effect (TGI: 31.9%); we also found BLU-667 treatment resulted in less pronounced antitumor response (30 mg/kg, BID, TGI: 50.0%) in MET amplified xenografts (Fig. 6B-E), which was consistent with the report that MET amplification reduced the sensitivity of BLU-667 [33]. Additionally, the combination of JC-010a and BLU-667 yielded profound tumor regression (Fig. 6B-E), with TGI value of 66.7%. And the combination treatment was well tolerated, as shown by the stable body weight (Fig. 6F). To gain insight into the mechanisms by which the combination treatment, we analyzed the tumors from mice, and our results revealed that both single and combination treatment reduced the expression of *p*-MEK, *p*-ERK, and *p*-AKT (Fig. 6G). Strikingly, tumors in JC-010a/BLU-667 group failed to grow after 8 days of treatment (Fig. 6C) and underwent robust apoptosis, which was evidenced by the elevation of apoptosis marker c-PARP (Fig. 6G). The toxicity in monotherapy and in combination treatment group was further analyzed by H&E staining, and there was no significant toxicity was found (Fig. 6H). Taken together, our data demonstrated that JC-010a impeded MET amplification-induced resistance to BLU-667 *in vivo*, and the combination of JC-010a and BLU-667 augmented the efficiency of BLU-667 through enhancing tumor apoptosis (Fig. 6I) to achieve durable antitumor response.

4. Discussion

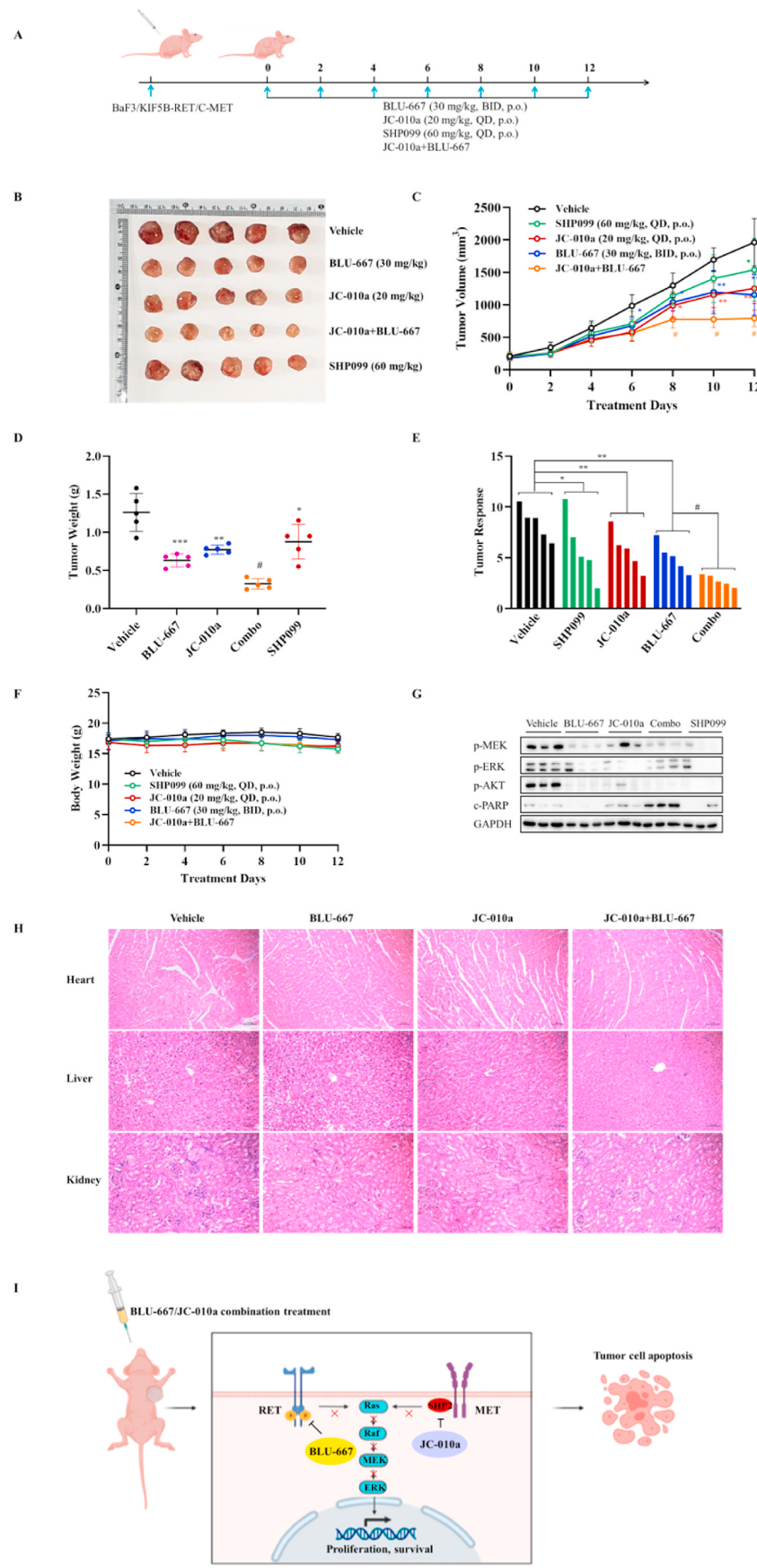
The aberrant activation of receptor tyrosine kinases (RTKs)/non-RTKs, such as EGFR, RET, BCR-ABL, and MET, are the most prevalent in human cancers. The oncogenic protein tyrosine phosphatase SHP2 can be recruited by these upstream RTKs/non-RTKs to regulate cancer development. Compared with tyrosine kinase inhibitors (TKIs), drug development for SHP2 inhibitors remains great challenge due to the polar and positively charged environment of the phosphatase active site [34]. Here, we reported a novel and selective SHP2 allosteric inhibitor JC-010a, which showed enhanced activity compared with SHP099. Our study demonstrated that JC-010a showed antiproliferation effect in multiple oncogene-addicted cancers, also the combination treatment of JC-010a with current targeted inhibitors could overcome RTK/non-RTK-mediated resistance (Fig. 7). In imatinib-resistant leukemia cells, we first revealed the novel role of SHP2 inhibitor by regulation the co-interaction of SHP2, BCR-ABL, and Hsp90, and our present study demonstrated that SHP2 inhibitors may be used as new therapeutic drugs for CML patients bearing BCR-ABL T315I mutation. In BLU-667-resistant RET-rearranged cancers, for the first time we proposed JC-010a/BLU-667 combination as a novel therapeutic approach to prolong anticancer response. Like many other SHP2 allosteric inhibitors in clinic (e.g. TNO155 and PF-07284892), JC-010a represented an appealing therapeutic agent for resistant cancers with EGFR^{T790M/C797S}, KRAS^{G12C} or alternate RTK activation, our present

study provided JC-010a as a novel broadly effective agent for clinical resistant cancers.

SHP2 is necessary for the full activation of RAS/Raf/ERK signaling pathway. KRAS is the most commonly mutated oncogene in this pathway, and strategies to target KRAS-mutant cancers with MEK inhibitors showed limited therapeutic benefits due to the induction of RTK genes and/or their ligands [17], such as FGFR1/2/3, EGFR/HER2, and MET [35]. SHP2 serves as the signal downstream of multiple RTKs, therefore, SHP2 inhibitor instead of various RTK inhibitors combination could inhibit adaptive resistance, which simplifies the treatment and reduced the risk of drug-drug interaction. As expected, we found JC-010a treatment attenuated the rebound of *p*-ERK and *p*-MEK mediated by RTK/SHP2 after selumetinib treatment (Fig. 2A-C and Fig. S1). Particularly, we found that JC-010a and selumetinib combination treatment exhibited the strongest synergy, which might attribute to JC-010a treatment could shift the KRAS-GTP to the KRAS-GDP state, resulting the dual inhibition of the RAS/MAPK. In this regard, future combination of JC-010a with KRAS^{G12C} inhibitor may also achieve prolonged antitumor response, as the current preclinical and clinical results revealed that some SHP2 allosteric inhibitors were effective in KRAS^{G12C} mutant cancers [36,37]. Due to the urgent need for new therapies in KRAS mutant patient, thus, combination therapies of JC-010a with MEK or KRAS^{G12C} inhibitors may provide promising therapeutic approaches to overcome drug resistance.

BCR-ABL-dependent resistances especially mediated by BCR-ABL T315I mutation have been accounted for about 20% of all the point mutations in CML [24], suggesting that BCR-ABL TKIs is unlikely to be universally effective. Due to the high positive correlations of SHP2 and BCR-ABL (Fig. 3A), we explored the effect of JC-010a on BCR-ABL T315I mutant cells, and our results revealed that JC-010a showed similar inhibition potency in imatinib-sensitive and imatinib-resistant cells (Fig. 3B and C); strikingly, JC-010a downregulated BCR-ABL and thereby inhibited its downstream signaling pathway (Fig. 3E), while SHP099 (5 μ M) did not decrease BCR-ABL expression (Fig. S5). We then explored the potential mechanisms of JC-010a regulating BCR-ABL expression. Our data demonstrated that inhibition of SHP2 by JC-010a destroyed the co-interaction between SHP2, BCR-ABL, and Hsp90, thereby leading to BCR-ABL degradation via caspase-dependent pathway (Fig. 3G and H). For the first time, we revealed the novel potential role of SHP2 inhibitor, that is, interrupting the interaction between BCR-ABL, Hsp90, and SHP2 may be critical to overcome BCR-ABL-dependent resistance in CML. Previous studies have shown that the steroidal glycoside SBF-1 [38] and PTP1B (a member of PTPs) inhibitors [39] promoted BCR-ABL degradation via disrupting the interaction between BCR-ABL and PTP1B, here, we revealed that regulation of SHP2 promoted BCR-ABL degradation. Our present data and previous reports mutually demonstrated that regulation of PTPs may be used as new approaches to overcome BCR-ABL T315I-mediated resistance in CML.

The most common resistance mechanisms in EGFR-driven NSCLC are the EGFR T790M/C797S mutation and the alternate RTK activation, which drive the resistance to gefitinib/erlotinib and osimertinib. JC-010a treatment can overcome two common resistance mechanisms (Fig. 4), which was consistent with the previous report that TNO155 abolished both EGFR mutation (T790M/C797S) and alternate RTK-mediated acquired resistance [40], as well as a recent report that



(caption on next page)

Fig. 6. Combined inhibition of RET and SHP2 prolongs antitumor response and overcomes resistance in MET amplified RET-rearranged xenograft tumors. (A) The administration plan in BaF3/KIF5B-RET/MET xenograft models. (B) Images of dissected tumor tissues ($n = 5$). (C) Tumor volume changes during experiment ($n = 5$). (D) After treatment, the mice were sacrificed, and the tumor tissues were weighed ($n = 5$). (E) Waterfall graph showing the response of xenografts treated with JC-010a, BLU-667, or both of drugs for 12 days ($n = 5$). (F) Body weight changes during the experiment ($n = 5$). (G) Western blotting analysis of *p-MEK*, *p-ERK*, *p-AKT*, and *c-PARP* in tumors ($n = 3$). (H) H&E staining of the heart, liver, and kidney ($n = 3$). (I) The related mechanisms of JC-010a overcome drug resistance in MET amplified RET-rearranged xenograft models. Data are presented as mean \pm SD. *** $P < 0.001$, ** $P < 0.01$, * $P < 0.05$, versus control group; # $P < 0.05$ versus JC-010a or BLU-667 group.

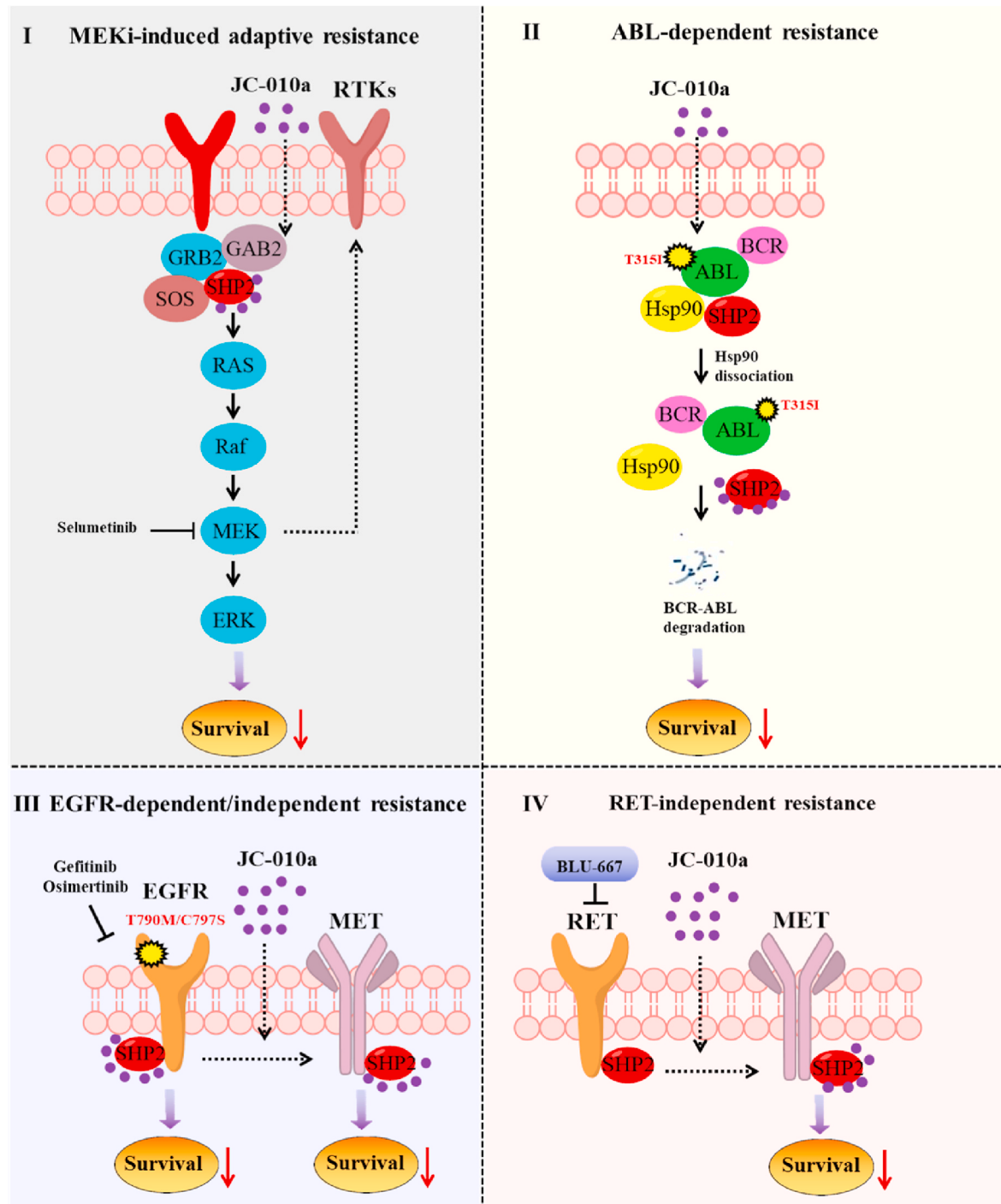


Fig. 7. A proposed model of JC-010a overcoming target therapy-induced resistance in different types of cancer. I, In KRAS mutant cancers, JC-010a can inhibit the reactivated RTK/SHP2/MAPK signaling pathway to overcome MEK inhibitor (MEKi)-induced adaptive resistance. II, In BCR-ABL T315I mutant leukemia cells, JC-010a disrupts the co-interaction between SHP2, BCR-ABL, and Hsp90 to overcome BCR-ABL^{T315I}-mediated resistance. III, In EGFR mutant (T790M and C797S) cancers, JC-010a can inhibit EGFR activation-mediated signals through SHP2. And JC-010a also abrogates alternated RTK (MET overexpression) activation-induced signaling pathway reactivation. IV, In RET-rearranged tumors where inhibition of RET results in compensatory activation of RTK (MET), JC-010a inhibits tumor growth by blocking the signaling downstream of MET through SHP2.

SHP2 allosteric inhibitor compound 129 inhibited proliferation of osimertinib-resistant NSCLC cells [41]. In addition to EGFR, RET rearrangements also serve as one of mechanisms for abnormal RTK activation in NSCLC. Recently, the newly approved selective RET TKIs (LOXO-292 and BLU-667) achieves encouraging efficacy in clinic, however, the development of acquired resistance limit the clinical benefit of RET TKIs. NSCLC, one of the typical models of oncogene addiction, which is highly dependent on various oncogenes, such as EGFR, RET, MET, and HER2, in this context, blocking one oncogenic driver results in the activation of other RTKs as alternative forces for continuous tumor growth. Here, we proposed a novel therapeutic strategy for RET-rearranged NSCLC to overcome resistance. We proved that combining SHP2 allosteric inhibitor JC-010a to inhibit the alternate MET activation-mediated MAPK activation through SHP2 was an effective therapeutic strategy (Fig. 5). Our data showed that JC-010a inhibited the proliferation of RET-rearranged cells and RET-rearranged cells bearing alternate RTK activation with similar potency; additionally, the combination treatment of JC-010a and BLU-667 achieved prolonged antitumor response compared with either single treatment (Fig. 5). This finding was further supported by *in vivo* results, in which JC-010a treatment inhibited tumor growth, and combination with BLU-667 caused sustained tumor regression and concomitantly triggered robust apoptosis (Fig. 6). As we known, this is the first report to show the application of SHP2 allosteric inhibitor in overcoming acquired resistance to RET selective inhibitor *in vitro* and *in vivo*. At present, several additional combination therapeutic approaches with allosteric SHP2 inhibitor have been proved with high efficiency in overcoming target agents-induced resistance. Leila et al. revealed that SHP099 in combination with ALK inhibitor ceritinib inhibited ALK-independent resistance towards ceritinib by preventing compensatory RAS/MAPK reactivation [42]. SHP099 could also inhibit MEK inhibitor-induced adaptive resistance by inhibiting KSR1 in KRAS-mutant gastric cancer [43]. Also, the clinical trial of KRAS^{G12C} inhibitor JDQ443 plus TNO155 showed robust antitumor activity in patient [44]. A recent clinical study revealed that the novel SHP2 allosteric inhibitor PF-07284892 abolished bypass signaling-mediated resistance to targeted therapy in multiple tumors [45]. At present, combinations of SHP2 allosteric inhibitor with MEK1/2, ERK1/2, ALK, EGFR, BRAF^{V600mut}, KRAS^{G12C}, and CDK4/6 inhibitors are currently being tested in the clinic [46]. All of these clinical and preclinical studies and our present data confirm that SHP2 inhibition is a broadly effective strategy to prevent or overcome clinical resistance to target therapy.

5. Conclusions

In conclusion, our present study identified JC-010a as a potent and selective SHP2 allosteric inhibitor, and our *in vitro* and *in vivo* results provide preclinical evidence for using JC-010a to overcome RTK/non-RTK-induced resistance towards TKIs or MAPK inhibitors. We demonstrated that in KRAS mutant cancer cells, JC-010a inhibited selumetinib-induced adaptive resistance through RTK/SHP2; in BCR-ABL T315I mutated CML, JC-010a disrupted the co-interaction between SHP2, BCR-ABL, and Hsp90, thereby overcoming BCR-ABL T315I-mediated imatinib resistance. In EGFR-driven NSCLC, JC-010a impeded both EGFR-dependent and EGFR-independent resistance to gefitinib and osimertinib. In RET-rearrangement cancers, JC-010a abrogated RET-independent resistance to BLU-667 both *in vitro* and *in vivo*. Taken together, our present study demonstrated that JC-010a was a novel effective SHP2 allosteric inhibitor and had great potential to be translated into clinically effective therapeutic drugs for resistant cancers.

Funding

This work was financially supported by National Key Research and Development Program of China (No.2023YFD2100604), Qingdao Marine Science and Technology Center (No.2022QNLM030003-1), Central

Government Guidance Funds for Local Scientific and Technological Development China (No.YDZX2023014), Qingdao Key Technology Research and Industrialization Demonstration (23-1-4-xxgg-13-nsh), and Qingdao Science and Technology Development Plan (No.21-1-6-gjxm-46-gx, No.22-3-6-gjxm-25-gx).

CRediT authorship contribution statement

Xuxiu Lu: Writing – original draft, Software, Data curation, Conceptualization. **Rilei Yu:** Visualization, Data curation, Conceptualization. **Zhen Li:** Validation, Investigation, Formal analysis. **Mengke Yang:** Validation, Formal analysis. **Jiajia Dai:** Methodology, Investigation, Formal analysis. **Ming Liu:** Writing – review & editing, Supervision, Project administration, Data curation.

Declaration of competing interest

The authors declare that they have no known competing financial interests or personal relationships that could have appeared to influence the work reported in this paper.

Acknowledgements

We thank Prof. Yuchao Gu from School of Medicine and Pharmacy, Ocean University of China, for his professional advice. We are grateful for Dr. Yajing Yang, Yanqing Wang, Qian Lin, and Ao Chen for technical assistance and reagent support.

Appendix A. Supplementary data

Supplementary data to this article can be found online at <https://doi.org/10.1016/j.canlet.2023.216517>.

References

- [1] A. Tulpule, J. Guan, D.S. Neel, H.R. Allegakoen, Y.P. Lin, D. Brown, et al., Kinase-mediated RAS signaling via membraneless cytoplasmic protein granules, *Cell* 184 (2021) 2649–2664 e2618.
- [2] R. Butti, S. Das, V.P. Gunasekaran, A.S. Yadav, D. Kumar, G.C. Kundu, Receptor tyrosine kinases (RTKs) in breast cancer: signaling, therapeutic implications and challenges, *Mol. Cancer* 17 (2018) 34.
- [3] M. Drosten, M. Barbacid, Targeting the MAPK pathway in KRAS-driven tumors, *Cancer Cell* 37 (2020) 543–550.
- [4] W.R. Montor, A.R.O.S.E. Salas, F.H.M.d. Melo, Receptor tyrosine kinases and downstream pathways as druggable targets for cancer treatment: the current arsenal of inhibitors, *Mol. Cancer* 17 (2018) 55.
- [5] R. Nussinov, C.J. Tsai, H. Jang, Anticancer drug resistance: an update and perspective, *Drug Resist. Updates* 59 (2021), 100796.
- [6] L. Huang, L. Fu, Mechanisms of resistance to EGFR tyrosine kinase inhibitors, *Acta Pharm. Sin. B* 5 (2015) 390–401.
- [7] T. O'Hare, C.A. Eide, M.W. Deininger, Bcr-Abl kinase domain mutations, drug resistance, and the road to a cure for chronic myeloid leukemia, *Blood* 110 (2007) 2242–2249.
- [8] K. Tang, M. Zhao, Y. Wu, Q. Wu, S. Wang, Y. Dong, et al., Structure-based design, synthesis and biological evaluation of aminopyrazines as highly potent, selective, and cellularly active allosteric SHP2 inhibitors, *Eur. J. Med. Chem.* 230 (2022), 114106.
- [9] A. Östman, C. Hellberg, F.D. Böhmer, Protein-tyrosine phosphatases and cancer, *Nat. Rev. Cancer* 6 (2006) 307–320.
- [10] R. Ren, Mechanisms of BCR-ABL in the pathogenesis of chronic myelogenous leukaemia, *Nat. Rev. Cancer* 5 (2005) 172–183.
- [11] J. Dai, Y. Zhang, Y. Gao, X. Bai, F. Liu, S. Li, et al., Toward a treatment of cancer: design and *in vitro/in vivo* evaluation of uncharged pyrazoline derivatives as a series of novel SHP2 inhibitors, *Int. J. Mol. Sci.* 23 (2022) 3497.
- [12] M.J. LaMarche, M. Acker, A. Argintaru, D. Bauer, J. Boisclair, H. Chan, et al., Identification of TNO155, an allosteric SHP2 inhibitor for the treatment of cancer, *J. Med. Chem.* 63 (2020) 13578–13594.
- [13] B. Czako, Y. Sun, T. McAfoos, J.B. Cross, P.G. Leonard, J.P. Burke, et al., Discovery of 6-[{(3S,4S)-4-Amino-3-methyl-2-oxa-8-azaspiro[4.5]decan-8-yl]-3-(2,3-dichlorophenyl)-2-methyl-3,4-dihydropyrimidin-4-one (IACS-15414), a potent and orally bioavailable SHP2 inhibitor, *J. Med. Chem.* 64 (2021) 15141–15169.
- [14] S.I. Ou, M. Koczwara, S. Ulahannan, P. Janne, J. Pacheco, H. Burris, et al., A12 the SHP2 inhibitor RMC-4630 in patients with KRAS-mutant non-small cell lung cancer: preliminary evaluation of a first-in-man phase 1 clinical trial, *J. Thorac. Oncol.* 15 (2020) S15–S16.

- [15] Y. Sun, B.A. Meyers, B. Czako, P. Leonard, F. Mseeh, A.L. Harris, et al., Allosteric SHP2 inhibitor, IACS-13909, overcomes EGFR-dependent and EGFR-independent resistance mechanisms toward osimertinib, *Cancer Res.* 80 (2020) 4840–4853.
- [16] R. Dong, M. Zhu, M. Liu, Y. Xu, L. Yuan, J. Bian, et al., EGFR mutation mediates resistance to EGFR tyrosine kinase inhibitors in NSCLC: from molecular mechanisms to clinical research, *Pharmacol. Res.* 167 (2021), 105583.
- [17] C. Fedele, H. Ran, B. Diskin, W. Wei, J. Jen, M.J. Geer, et al., SHP2 inhibition prevents adaptive resistance to MEK Inhibitors in multiple cancer models, *Cancer Discov.* 8 (2018) 1237–1249.
- [18] J.T. Bagdanoff, Z. Chen, M. Acker, Y.N. Chen, H. Chan, M. Dore, et al., Optimization of fused bicyclic allosteric SHP2 inhibitors, *J. Med. Chem.* 62 (2019) 1781–1792.
- [19] X. Lu, L. Qin, M. Guo, J. Geng, S. Dong, K. Wang, et al., A novel alginate from *Sargassum* seaweed promotes diabetic wound healing by regulating oxidative stress and angiogenesis, *Carbohydr. Polym.* 289 (2022), 119437.
- [20] C.J. Caunt, M.J. Sale, P.D. Smith, S.J. Cook, MEK1 and MEK2 inhibitors and cancer therapy: the long and winding road, *Nat. Rev. Cancer* 15 (2015) 577–592.
- [21] J.C. Hunter, A. Manandhar, M.A. Carrasco, D. Gurbani, S. Gondi, K.D. Westover, Biochemical and structural analysis of common cancer-associated KRAS mutations, *Mol. Cancer Res.* 13 (2015) 1325–1335.
- [22] A. Quintás-Cardama, J. Cortes, Molecular biology of BCR-ABL1-positive chronic myeloid leukemia, *Blood* 113 (2009) 1619–1630.
- [23] H. Rui, K. Qian, L. Huimin, L. Yuhua, New insights into the molecular resistance mechanisms of chronic myeloid leukemia, *Curr. Cancer Drug Targets* 16 (2016) 323–345.
- [24] T.P. Braun, C.A. Eide, B.J. Druker, Response and resistance to BCR-ABL1-targeted therapies, *Cancer Cell* 37 (2020) 530–542.
- [25] D. Zeng, M. Gao, R. Zheng, R. Qin, W. He, S. Liu, et al., The HSP90 inhibitor KW-2478 depletes the malignancy of BCR/ABL and overcomes the imatinib-resistance caused by BCR/ABL amplification, *Exp. Hematol. Oncol.* 11 (2022) 33.
- [26] X. Lu, J. Geng, J. Zhang, J. Miao, M. Liu, Xanthohumol, a prenylated flavonoid from hops, induces caspase-dependent degradation of oncoprotein BCR-ABL in K562 cells, *Antioxidants* 8 (2019) 402.
- [27] S.M. Lim, N.L. Syn, B.C. Cho, R.A. Soo, Acquired resistance to EGFR targeted therapy in non-small cell lung cancer: mechanisms and therapeutic strategies, *Cancer Treat. Rev.* 65 (2018) 1–10.
- [28] A. Leonetti, S. Sharma, R. Minari, P. Perego, E. Giovannetti, M. Tiseo, Resistance mechanisms to osimertinib in EGFR-mutated non-small cell lung cancer, *Br. J. Cancer* 121 (2019) 725–737.
- [29] M.J. Niederst, J.A. Engelman, Bypass mechanisms of resistance to receptor tyrosine kinase inhibition in lung cancer, *Sci. Signal.* 6 (2013) re6.
- [30] C. Romei, R. Ciampi, R. Elisei, A comprehensive overview of the role of the RET proto-oncogene in thyroid carcinoma, *Nat. Rev. Endocrinol.* 12 (2016) 192–202.
- [31] K.Z. Thein, V. Velcheti, B.H.M. Mooers, J. Wu, V. Subbiah, Precision therapy for RET-altered cancers with RET inhibitors, *Trends Cancer* 7 (2021) 1074–1088.
- [32] J.J. Lin, S.V. Liu, C.E. McCoach, V.W. Zhu, A.C. Tan, S. Yoda, et al., Mechanisms of resistance to selective RET tyrosine kinase inhibitors in RET fusion-positive non-small-cell lung cancer, *Ann. Oncol.* 31 (2020) 1725–1733.
- [33] V. Subbiah, J.F. Gainor, R. Rahal, J.D. Brubaker, J.L. Kim, M. Maynard, et al., Precision targeted therapy with BLU-667 for RET-driven cancers, *Cancer Discov.* 8 (2018) 836–849.
- [34] L. M.Scott, H. R.Lawrence, S. M.Sefti, N. J.Lawrence, J. Wu, Targeting protein tyrosine phosphatases for anticancer drug discovery, *Curr. Pharmaceut. Des.* 16 (2010) 1843–1862.
- [35] H. Lu, C. Liu, R. Velazquez, H. Wang, L.M. Dunkl, M. Kazic-Legueux, et al., SHP2 inhibition overcomes RTK-mediated pathway reactivation in KRAS-mutant tumors treated with MEK inhibitors, *Mol. Cancer Therapeut.* 18 (2019) 1323–1334.
- [36] A.M. Taylor, B.R. Williams, F. Giordanetto, E.H. Kelley, A. Lescarbeau, K. Short sleeves, et al., Identification of GDC-1971 (RLY-1971), a SHP2 inhibitor designed for the treatment of solid tumors, *J. Med. Chem.* 66 (2023) 13384–13399.
- [37] Q. Hou, W. Jiang, W. Li, C. Huang, K. Yang, X. Chen, et al., Identification of a novel, potent, and orally bioavailable guanidine-based SHP2 allosteric inhibitor from virtual screening and rational structural optimization for the treatment of KRAS mutant cancers, *J. Med. Chem.* 66 (2023) 13646–13664.
- [38] A. Elgehama, W. Chen, J. Pang, S. Mi, J. Li, W. Guo, et al., Blockade of the interaction between Bcr-Abl and PTB1B by small molecule SBF-1 to overcome imatinib-resistance of chronic myeloid leukemia cells, *Cancer Lett.* 372 (2016) 82–88.
- [39] D. Alvira, R. Naughton, L. Bhatt, S. Tedesco, W.D. Landry, T.G. Cotter, Inhibition of protein-tyrosine phosphatase 1B (PTP1B) mediates ubiquitination and degradation of Bcr-Abl protein, *J. Biol. Chem.* 286 (2011) 32313–32323.
- [40] C. Liu, H. Lu, H. Wang, A. Loo, X. Zhang, G. Yang, et al., Combinations with allosteric SHP2 inhibitor TNO155 to block receptor tyrosine kinase signaling, *Clin. Cancer Res.* 27 (2021) 342–354.
- [41] R. Luo, W. Fu, J. Shao, L. Ma, S. Shuai, Y. Xu, et al., Discovery of a potent and selective allosteric inhibitor targeting the SHP2 tunnel site for RTK-driven cancer treatment, *Eur. J. Med. Chem.* 253 (2023), 115305.
- [42] L. Dardaei, H.Q. Wang, M. Singh, P. Fordjour, K.X. Shaw, S. Yoda, et al., SHP2 inhibition restores sensitivity in ALK-rearranged non-small-cell lung cancer resistant to ALK inhibitors, *Nat. Med.* 24 (2018) 512–517.
- [43] W. Zheng, Z. Yang, P. Song, Y. Sun, P. Liu, L. Yue, et al., SHP2 inhibition mitigates adaptive resistance to MEK inhibitors in KRAS-mutant gastric cancer through the suppression of KSR1 activity, *Cancer Lett.* 555 (2023), 216029.
- [44] A. Weiss, E. Lorthiois, L. Barys, K.S. Beyer, C. Bonino-Confaglia, H. Burks, et al., Discovery, preclinical characterization, and early clinical activity of JDQ443, a structurally novel, potent, and selective covalent oral inhibitor of KRASG12C, *Cancer Discov.* 12 (2022) 1500–1517.
- [45] A. Drilon, M.R. Sharma, M.L. Johnson, T.A. Yap, S. Gadgeel, D. Neupert, et al., SHP2 inhibition sensitizes diverse oncogene-addicted solid tumors to re-treatment with targeted therapy, *Cancer Discov.* 13 (2023) 1789–1801.
- [46] N.M. Sodir, G. Pathria, J.I. Adamkewicz, E.H. Kelley, J. Sudhamsu, M. Merchant, et al., SHP2: a pleiotropic target at the interface of cancer and its microenvironment, *Cancer Discov.* (2023) OF1–OF17.